

A Novel Adaptive Fuzzy MPPT Algorithm under Changing Atmospheric Conditions

Zhang Yan¹, Wang Ya-Jun², Chang Jia-Bao³

¹Power Electronics and Power Drives, Liaoning University of Technology, China

²Professor, Department of Electronic and Information Engineering, Liaoning University of Technology, China

³Liaoning University of Technology, Electronics and Communication Engineering, China

E-mail: ¹279919941@qq.com

Abstract

The paper aims at the incompatibility between the speed and stability of the traditional MPPT algorithm and the imprecise search of the fuzzy control algorithm. An improved photovoltaic adaptive fuzzy control MPPT algorithm is proposed in this thesis. The solar irradiance changes dramatically and hence four kinds of fuzzy control algorithms with different input are modeled and simulated. The results indicate that the proposed fuzzy control algorithm using slope and slope change rate of P-U curve as input is the best. On this basis, dP/dU and duty cycle $D(n-1)$ at $n-1$ moment are used as input to improve the tracking speed and optimal range. At the same time using shrinkage factor $1/I*|dP/dU|$ real-time adjustment of $D(n-1)$ further shortens the optimal time of the algorithm. The algorithm is simulated and applied in a block. Simulation results show that the proposed algorithm is superior to the fuzzy control algorithm in steady-state oscillation rate, tracking speed and efficiency, and the algorithm is simple and easy to implement.

Keywords: MPPT, photovoltaic power generation, maximum power tracing, fuzzy control, Boost

1. Introduction

As the reserves of traditional fossil fuels decrease year by year, countries have begun to vigorously develop efficient and clean renewable energy. Since 2017, the world's installed non-fossil energy capacity has grown by about 25% annually. Photovoltaic power generation is widely used in all walks of life because of its pollution-free, renewable and wide application. The PV characteristics curve is highly nonlinear and the efficiency is greatly influenced by

irradiation and temperature. Therefore, it is indispensable to propose an efficient, simple and universal MPPT algorithm[1-3]

At present, maximum power tracking technology (MPPT) mainly includes traditional MPPT tracking methods, such as Short-Circuit Current method, increment conductance algorithm (INC), perturbation and observation algorithm (P&O), table lookup method and intelligent control methods [4] such as Artificial Neural Network (ANN), Particle Swarm Optimization (PSO), fuzzy control (FLC) and cuckoo algorithm (CS). Moreover, the traditional MPPT algorithm is cost efficient, easy to execute, stable accuracy and tracking speed cannot be considered simultaneously [5]. Although artificial neural network is used to deal with nonlinear system, it requires too much data and too long training time, making it impractical. Particle swarm optimization has strong global search ability, but often falls into local optimal solution. Compared with traditional MPPT algorithm, artificial neural network and particle swarm optimization, fuzzy control has lower output power fluctuation and stronger system robustness and fault tolerance. Therefore, the research of photovoltaic power generation system mostly opts intelligent control methods.[6]

Focusing on the problem, the fuzzy rules and input and output variables of PV MPPT are optimized in this dissertation. In this proposed Fuzzy algorithm, dP/dU and duty ratio $D(n-1)$ at the previous moment are selected as error E and error change rate EC respectively, and duty ratio $D(n)$ is selected as output to avoid large fluctuation of output power of traditional disturbance observation method, and also takes into account the characteristics of traditional fuzzy algorithm with wide searching range and high efficiency of artificial neural network. The tracking speed, steady-state oscillation rate and power fluctuation of MPPT algorithm are improved to a certain extent. It improves the conversion rate of photovoltaic power generation.

The core content of this dissertation is as follows:

- (1) Aims at the problems of traditional fuzzy controller, such as low stability precision and large steady oscillation rate. $D(n-1)$ was selected as the input to improve the optimization range and search ability of photovoltaic system.
- (2) Under changing atmospheric conditions, the traditional fuzzy controller can't track the maximum power point. So this dissertation uses the shrinkage factor $1/I*|dP/dU|$ implementation to adjust $D(n-1)$, the maximum power point of PV system in real-time tracking.

2. Photovoltaic Cell Mathematical Model and Illumination Parameters

2.1 Photovoltaic Cell Characteristics

Photovoltaic cell model can be simplified to photodiode model [7]. The corresponding circuit of PV module is shown in Figure 1.

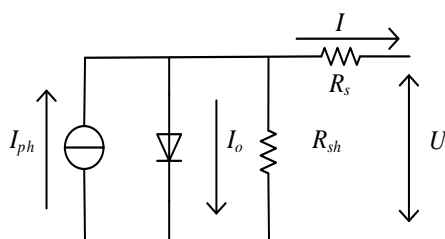


Figure 1. Corresponding circuit of photovoltaic cell

PV model output current equation is expressed as:

$$I = I_{pv} - I_0 \left\{ \exp \left[\frac{q(U+R_s \times I)}{AKT} \right] - 1 \right\} - \frac{U+R_s \times I}{R_{sh}} \quad (1)$$

Among them, R_s is a series resistance, generally only a few ohms; R_{sh} is a shunt resistance, typically about a few thousand ohms; I is the output current of the PV model; U is the output voltage of the photovoltaic cell; I_{ph} is the photocurrent; I_0 is the saturation current; A is the diode ideal parameter, generally A is in the range of 1~2; K is Boltzmann's constant, $K=1.38 \times 10^{-23}$ J/K; q is the charge parameter, $q=1.6 \times 10^{-19}$ C; T is temperature of the PV model, expressed in °C [8].

When the PV module is working under standard conditions (irradiation $S_{ref}=1000$ W/m², Temperature for 25 °C) formula (1) is obtained. As PV modules are greatly affected by environmental factors, it is impossible to ensure that the working environment is always standard. Reference parameters need to be adjusted and modified as follows:

$$\Delta S = \frac{S}{S_{ref}} - 1 \quad (2)$$

$$\Delta T = T - T_{ref} \quad (3)$$

$$I_{sc} = I_{sc}(1 + a\Delta T) \times \frac{S}{S_{ref}} \quad (4)$$

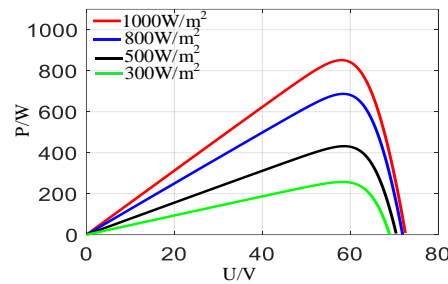
$$V_{oc} = V_{oc}(1 - c\Delta T) \times \ln(e + b\Delta S) \quad (5)$$

$$I_{mm} = I_m(1 + a\Delta T) \times \frac{S}{S_{ref}} \quad (6)$$

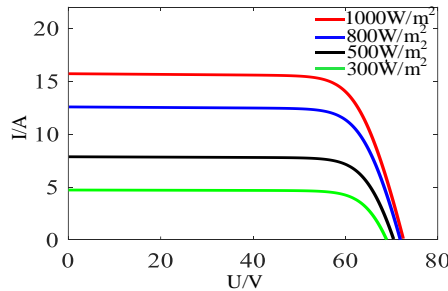
$$V_{mm} = V_m(1 - c)\Delta T \times \ln(e + b\Delta S) \quad (7)$$

In the formula: a , b , c are the corrected parameters, $a = 0.0027 \text{ } ^\circ\text{C}$, $b = 0.0006 \text{ (W/m}^2\text{)}$, $c = 0.00275 \text{ } ^\circ\text{C}$. I_{sc} , V_{oc} , I_{mm} , V_{mm} are the modified parameters.

According to the calculation and analysis of the above formula, the number of parallel and series PV model is 2, choosing 1Soltecg 1SB-215-P as PV module. Figure 2(a) shows P-U characteristic curve under different irradiation. The P-V characteristic curve of PV model is single-peak curve, that is, there is one extreme power point. Figure 2(b) is the I-V characteristic curve under different temperature conditions. PV modules have strong nonlinear characteristics, that is, the short circuit current fluctuates violently [9-10].



(a) P-V characteristic curve of PV model under different irradiation



(b) I-V characteristic curve of PV model under different irradiation

Figure 2. PV model characteristic curves

2.2 Lighting Parameters

The average light intensity of a middle and low-density block in one week is about $200 \text{ W/m}^2 \sim 700 \text{ W/m}^2$, and the annual light intensity of this area is mainly concentrated about $300 \text{ W/m}^2 \sim 1000 \text{ W/m}^2$. The relationship between the corresponding time and light intensity parameters in a day and simulation time is displayed in Table 1.

Table 1. Irradiation simulation parameters

simulation time/s	0-0.3	0.3-0.5	0.5-0.75	0.75-1
Local time	0:00 am— 5:00 am	5:00 am— 8:00 am	8:00 am— 10:00 am	10:00 am— 14:00 pm
Illumination intensity(W/m ²)	0	337.43	532.32	1035.43
Simulation time/s	1-1.25	1.25-1.5	1.5-1.8	—
Local time	14:00 pm— 16 :00 pm	16:00 pm— 18:00 pm	18:00 pm— 24:00 pm	—
Illumination intensity(W/m ²)	543.22	280.43	0	—

3. Fuzzy Controller

The realization of fuzzy controller depends on the domain division, membership degree and fuzzy quantity. Therefore, in view of the incompatibility between tracking speed and stable accuracy of traditional MPPT algorithm, fuzzy control algorithm is adopted in this dissertation to convert tracking of MPP points into soft computing and the average efficiency can reach about 97%. Hence it is widely used in photovoltaic power generation [11-12].

3.1 Traditional Fuzzy Controller

Figure 3 represents the schematic diagram of Boost circuit simulation under fuzzy control. Firstly, the voltage and current of photovoltaic cells are sampled, the error(E) and error change rate (EC) signal are calculated. Secondly, intelligent reasoning of expert system is realized by fuzzy controller (fuzzier, fuzzy algorithm and defuzzification). Then, Mamdani reasoning and the aggregation of rule base are used to obtain the set of Boolean logic. Finally, the accurate duty cycle D is obtained by solution center of gravity method (COA), and the error free control is realized [13-15].

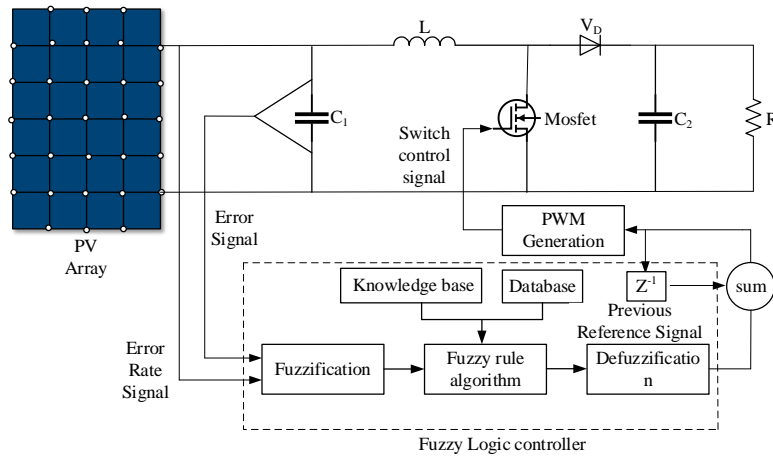


Figure 3. Fuzzy control algorithm block diagram

The input E , EC and output $D(n)$ of fuzzy controller are divided into the following 7 elements: $E, EC \in \{NB, NM, NS, ZE, PS, PM, PB\}$, $D(n) \in \{NB, NM, NS, PS, PM, PB\}$, NL is negative large, NM is negative medium, NS is negative small, $Z0$ is zero, PS is positive small, PM is medium, and PL is positive large [15-16].

This paper adopts four kinds of fuzzy control, namely type I, II, III and IV respectively. At the same time, the above output signals are duty cycle $D(n)$. type I fuzzy control input for the $dP=P(n)-P(n-1)$ and the $dU=U(n)-U(n-1)$, type II input is $E=dP/dU$ and $EC=E(n)-E(n-1)$, type III input is $E=dP/dI$ and $EC=E(n)-E(n-1)$, type IV input is $E=dP/dU$, and $EC=P(n)-P(n-1)$. Triangle and bell-shaped membership functions are used for type I, II, III and IV, and then the fuzzy control 3D surface diagram is obtained by setting fuzzy rules, as shown in Figure 4. Figure 4(a) is a three-dimensional diagram of type I fuzzy control, $dP > 0$ and $dU > 0$, $D(n)$ decreased; $dP > 0$ and $dU < 0$, $D(n)$ increased; When $dP < 0$ and $dU < 0$, $D(n)$ decreases; $dP < 0$ and $dU > 0$, $D(n)$ increases. Figure 4(b) and (c) are three-dimensional diagrams of type II and type III fuzzy control respectively. Figure 4(b) and (c) are three-dimensional diagrams of type II and type III fuzzy control respectively. The core ideas of type II and type III are basically the same, that is, $E > 0$ and $EC > 0$, and $D(n)$ decreases. $E > 0$ and $EC < 0$, $D(n)$ decreased; $E < 0$ and $EC > 0$, $D(n)$ increased; $E < 0$ and $EC < 0$, $D(n)$ decreases. Figure 4(d) shows the 3D diagram of type IV fuzzy control, $E > 0$ and $EC > 0$, and $D(n)$ decreases. $E > 0$ and $EC < 0$, $D(n)$ decreased; $E < 0$ and $EC > 0$, $D(n)$ increased; $E < 0$ and $EC < 0$, $D(n)$ decreases [16-20].

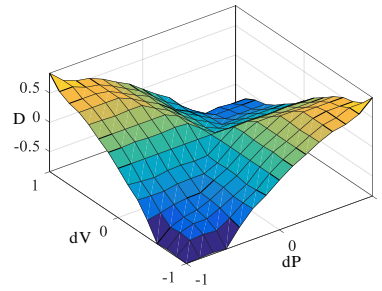


Figure 4 (a). 3D surface diagram of type I fuzzy control

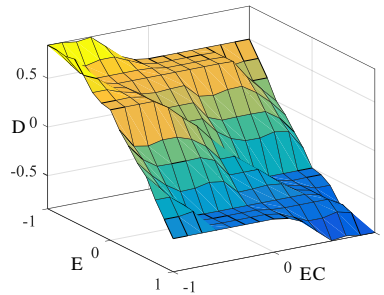


Figure 4 (b). 3D surface diagram of type II fuzzy control

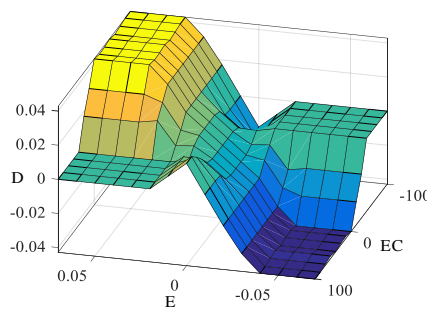


Figure 4 (c). 3D surface diagram of type III fuzzy control

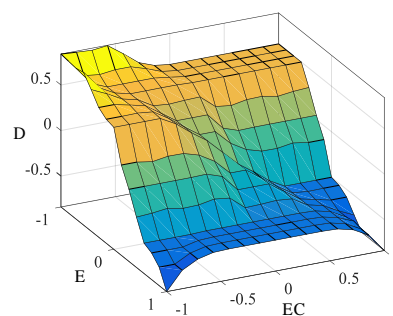


Figure 4 (d). 3D surface diagram of type IV fuzzy control

Figure 4. 3D surface diagram of type I, II, III and IV fuzzy control

3.2 Proposed Algorithm

Solving the problems of power fluctuation and tracking speed existing in the traditional fuzzy control MPPT algorithm, a novel adaptive fuzzy photovoltaic MPPT algorithm is

proposed. The process is displayed in Figure 5. The method selects dP/dU and duty cycle disturbance step $D(n-1)$ at $n-1$ moment as input, meanwhile the final signal is still $D(n)$. The input and output membership function (gbellmf and trimf) variables are established by Matlab/Simulink to achieve MPPT tracking.

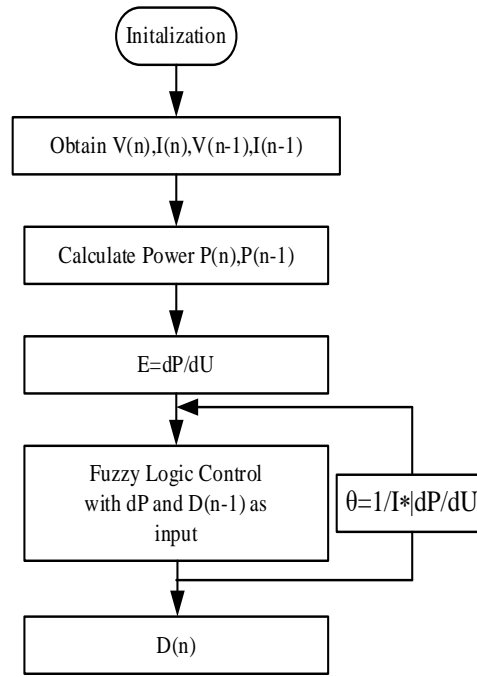


Figure 5. Fuzzy control algorithm flow chart

As the characteristic curve of photovoltaic cell fluctuates greatly with external conditions and has strong nonlinear characteristics, the shape and position of membership function are asymmetric. Membership function is displayed in Figure 6. Zadeh method and Mamdani method are commonly used in fuzzy control. Mamdani inference mechanism has optimized fuzzy system and compactly approximated continuous function, and hence Mamdani reasoning is adopted. The area center method was employed in the clearness process, and the continuous membership function was calculated by MAX-MIN compound calculation. Figure 7 for $|dP/dU|$ and contraction factor θ change with the light intensity curve. As shown in Figure 7, the step length contraction factor and $|dP/dU|$ changes small ripple and had higher two curve fitting degree, so the selection made is contraction factor. Once the tracking point is more than maximum power point, after rising exponentially, it increases the complexity of the system and at the same time will also slow down the tracking speed, and the normalization processing should be carried out.

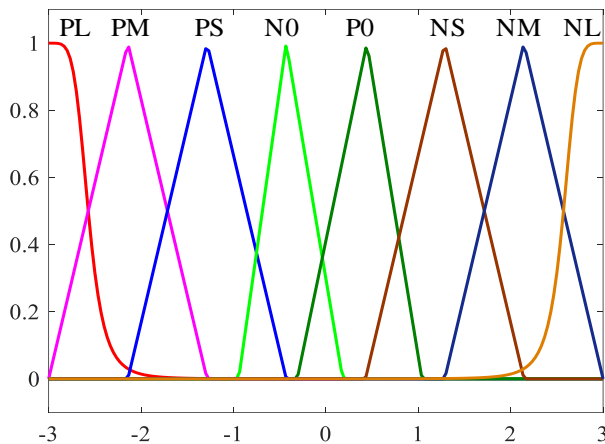


Figure 6 (a). dP/dU

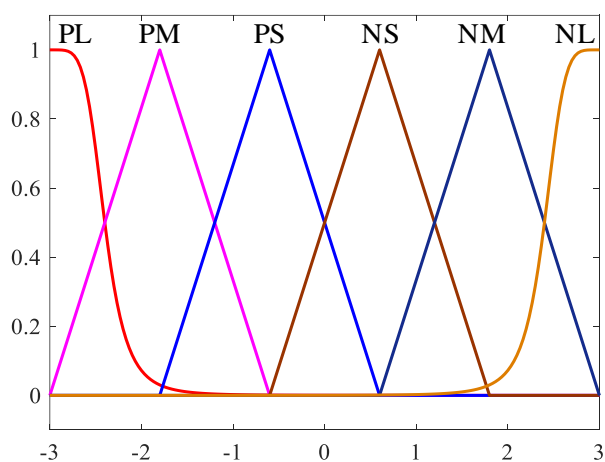


Figure 6 (b). $D(n-1)$

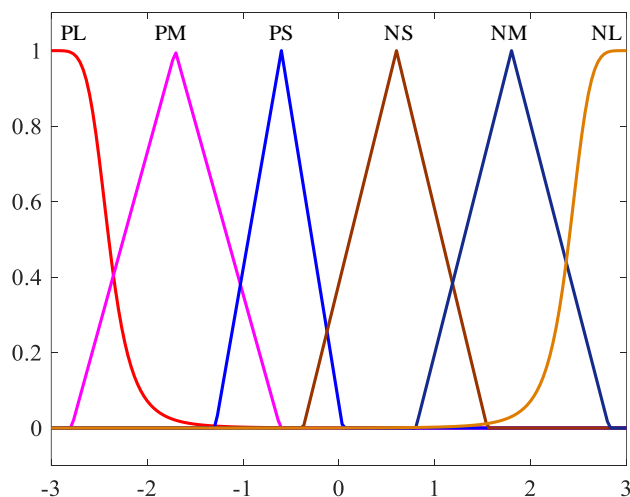


Figure 6 (c). $D(n)$

Figure 6. Membership function of fuzzy logical controller

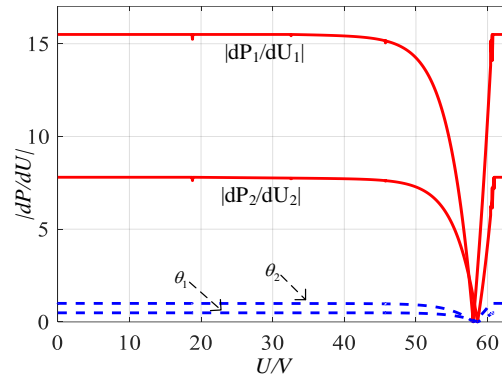


Figure 7. $|dP/dU|$ and θ Characteristic curve

The characteristic curve of photovoltaic cells is nonlinear. Through the study of disturbance observation method, traditional fuzzy control and P-U characteristic curve, the control logic rules are as follows.

1. $dP/dU > 0$, $D(n-1) > 0$, far from the maximum power point, then $D(n)$ decreases in the opposite direction;
2. $dP/dU > 0$, $D(n-1) < 0$, close to the maximum power point, then $D(n)$ increases in the original direction;
3. $dP/dU < 0$, $D(n-1) < 0$, far from the maximum power point, then $D(n)$ increases in the original direction;
4. $dP/dU < 0$, $D(n-1) > 0$, close to the maximum power point, then $D(n)$ decreases in the opposite direction;
5. Photovoltaic power generation systems need to respond quickly to the changes in the irradiation and temperature.

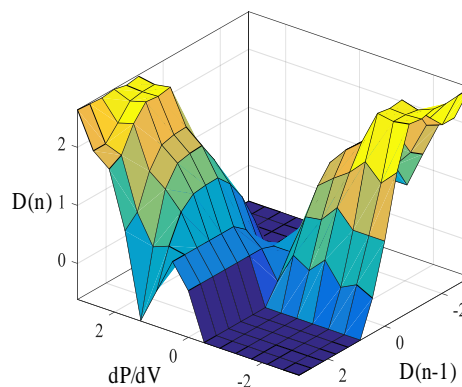


Figure 8. Proposed three-dimensional surface diagram of fuzzy control

In order to give consideration to the above principles, fuzzy control adopts A and B then C inference statements. The final fuzzy controller rules are shown in Table 2 and the 3D curve of fuzzy control is shown in Fig. 8.

Table 2. Fuzzy controller rules

dP/dV	D(n-1)					
	D(n)	NL	N M	NS	PS	PM
NL	PL	PL	PM	NS	NS	NS
NM	PL	PM	PS	NS	NS	NS
NS	PS	PM	PM	NS	NS	NS
NO	PS	PS	PS	NS	NS	NS
P0	NS	NS	NS	PS	PS	PS
PS	NS	NS	NS	PM	PM	PS
PM	NS	NS	NS	PS	PM	PL
PL	NS	NS	NS	PM	PB	PL

4. Simulation Results and Discussion

The BOOST circuit is simulated and tested under Matlab/Simulink. The simulation circuit is displayed in Figure 9. Simulation parameters can be seen in Table 1 and Table 3 shows BOOST simulation circuit parameters. The simulation duration is 1.8s. Ode23 (Bogacki-Shampine) is used as the algorithm.

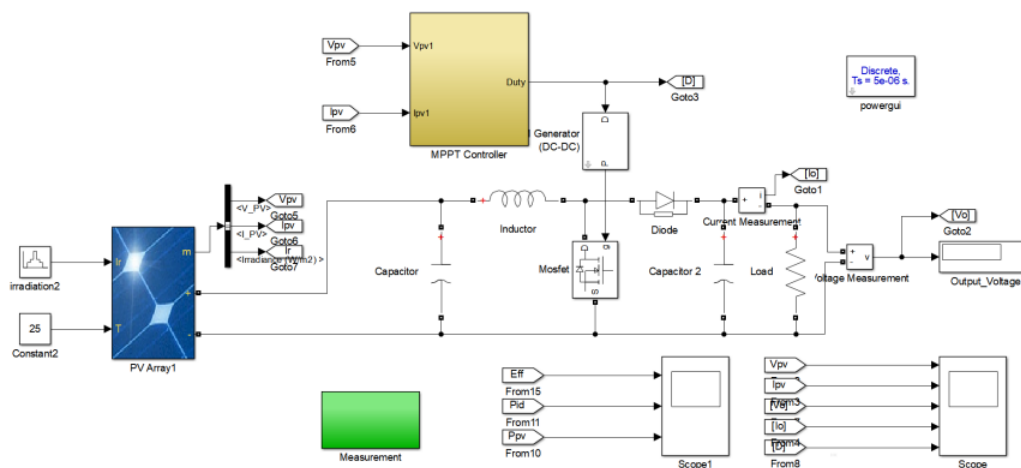


Figure 9. System simulation model under Matlab/Simulink

The simulated light intensity is shown in Figure 10 (a) : 0s~0.3s, $S = 0 \text{ W/m}^2$; 0.3s~0.5s, $S = 300 \text{ W/m}^2$; 0.5s~0.75s, $S = 500 \text{ W/m}^2$; 0.75s~1s, $S = 1000 \text{ W/m}^2$. After 0.25s, the light intensity gradually changes into 500 W/m^2 , 300 W/m^2 and 0 W/m^2 . The type I, II, III and IV fuzzy control algorithms are compared, and the output voltage, output current, output power, efficiency and duty cycle are simulated respectively. The results are displayed in figure 10(b)-(f).

Table 3. Parameters of photovoltaic module and BOOST circuit under standard

Photovoltaic cell parameters	The values	BOOST circuit parameters	The values
Open circuit voltage U_{oc}/V	72.6	Input capacitance $C_1/\mu\text{F}$	100
Short circuit current I_{sc}/A	15.68	Boost inductance L/mH	2
Maximum power point voltage U_{mp}/V	58	Output resistance R/Ω	20
Maximum power point current I_{mp}/A	14.7	Output capacitance $C_1/\mu\text{F}$	100
Temperature coefficient	-0.36099	——	——
Temperature coefficient	0.102	——	——
The most powerful P_m/W	852.3	——	——

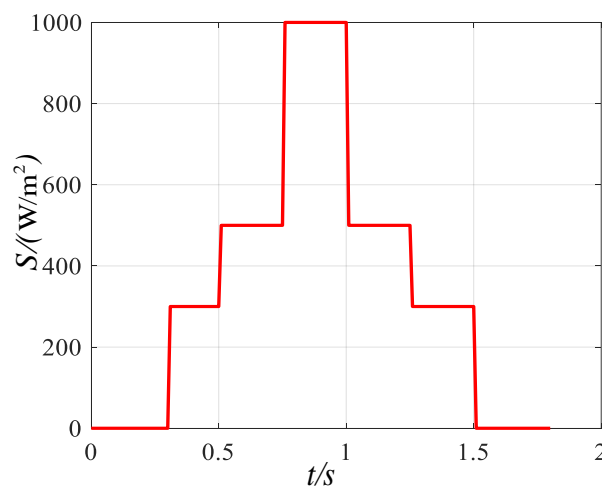


Figure 10 (a). Waveform of light intensity

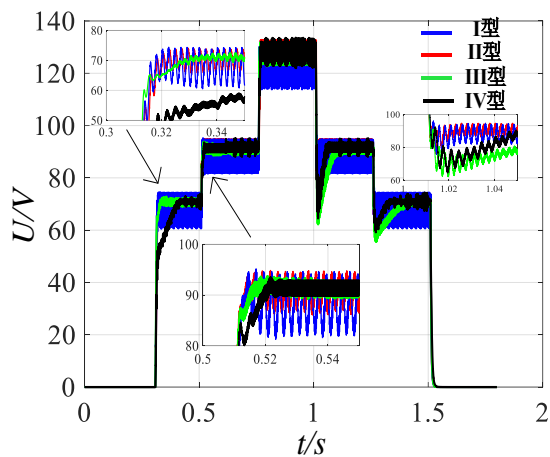


Figure 10 (b). Type I, II, III and IV output voltage waveform

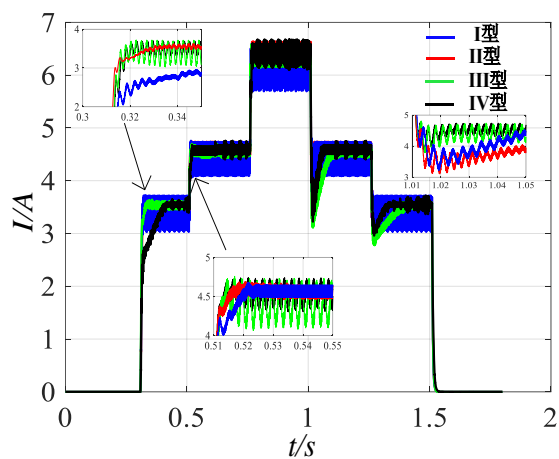


Figure 10 (c). Type I, II, III and IV output current waveform

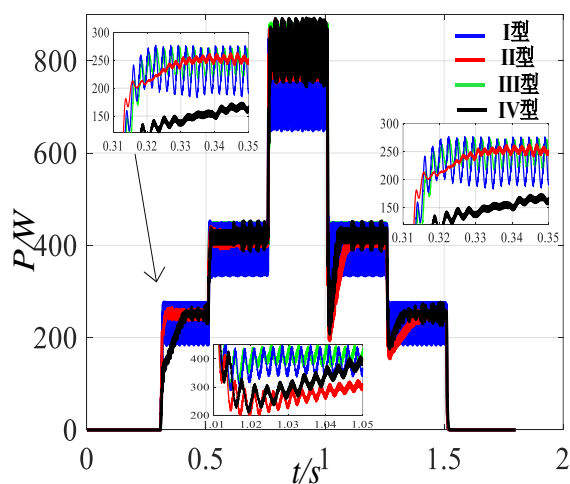


Figure 10 (d). Type I, II, III and IV output power waveform

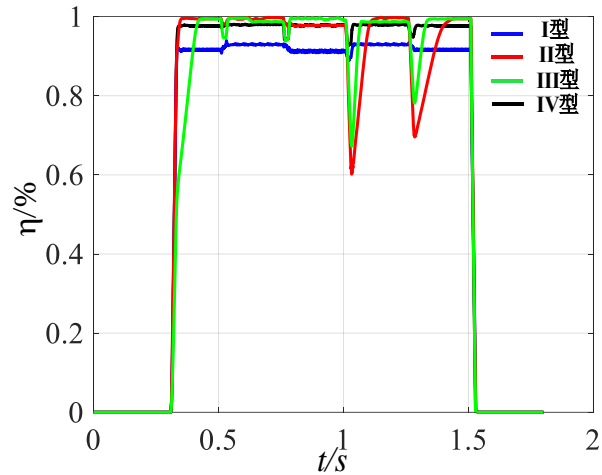


Figure 10 (e). Type I, II, III and IV output Efficiency waveform

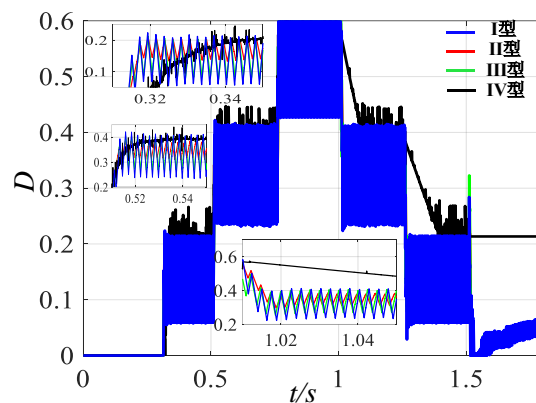


Figure 10 (f). Type I, II, III and IV duty cycle waveform

Figure 10. Simulation results of four kinds of fuzzy control

As displayed in Fig.10(b)-(f), the output voltage U , output current I , output power P , efficiency η and duty cycle D of the type II fuzzy control algorithm, within one day has small steady-state error, small system inertia, fast tracking speed and high conversion efficiency. Type III fuzzy control adopts the slope and slope change rate of I-P characteristic curve of photovoltaic cells as input, and the optimization width of I-dP /dI characteristic curve is about 63% of that of type II control algorithm, which indirectly limits the accuracy and stability of type III fuzzy control. According to the characteristic curve of photovoltaic cells, the slope and power difference of P-U characteristic curve are used as the input of type IV fuzzy control. Although the sampling is simple and the searching range is wide, the setting requirements of main circuit parameters and rule base are strict, and it is likely to fall within three-point search. The type I fuzzy control adopts voltage difference and power difference as input. The algorithm has simple idea and fast optimization speed, but it lacks the optimal boundary point for dividing

the characteristic curve of photovoltaic cells. The sharpening process lacks accuracy and has large steady-state error. Type II fuzzy control adopts the slope and slope change rate of PV cell P-U characteristic curve as input. The slope change by the left of MPP is not obvious, hence the fuzzy process is not precise. Therefore, the performance of this algorithm still has room for improvement. To sum up, the performance of photovoltaic power generation fuzzy system mainly depends on the optimization range, conversion efficiency, tracking speed, stability error and system inertia.

The proposed fuzzy control algorithm is compared with the type II fuzzy control, and the output voltage, output current, output power, efficiency and duty cycle are simulated respectively. The results are displayed in fig.11 (a)-(e).

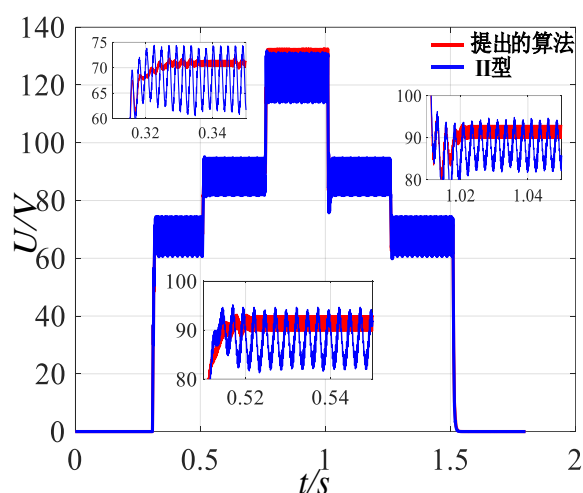


Figure 11 (a). Output voltage contrast diagram of the proposed fuzzy algorithm and type II fuzzy algorithm in one day

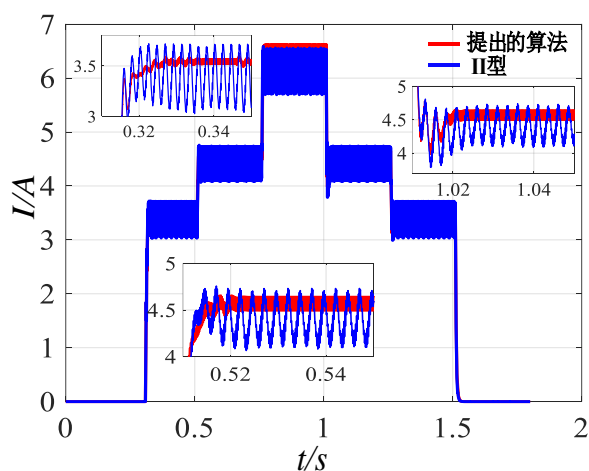


Figure 11 (b). Output current comparison of the proposed fuzzy algorithm and the type II fuzzy algorithm in one day

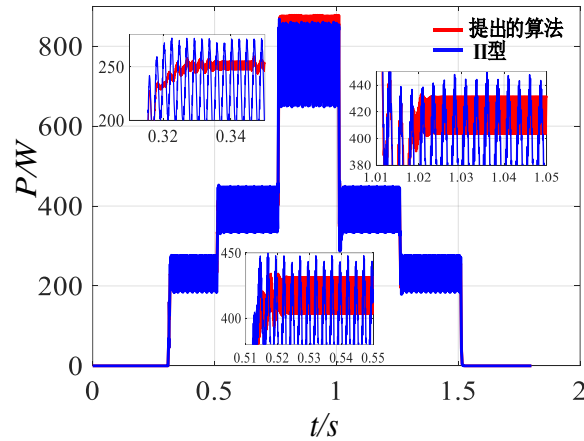


Figure 11 (c). Output power comparison of the proposed fuzzy algorithm and type II fuzzy algorithm in one day

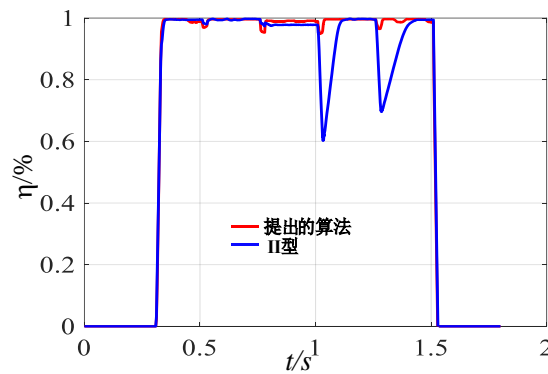


Figure 11 (d). Comparison of output efficiency between the proposed fuzzy algorithm and type II fuzzy algorithm in one day

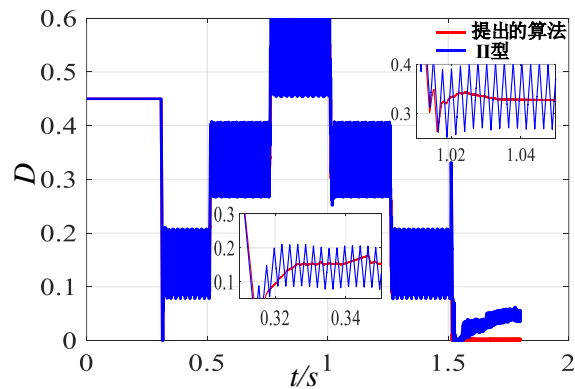


Figure 11 (e). Duty cycle comparison of the proposed fuzzy algorithm and type II fuzzy algorithm in one day

Figure 11. Comparison of simulation results between the proposed fuzzy algorithm and type II fuzzy algorithm

As shown in fig.11(a)-(e), all parameters of the proposed fuzzy algorithm are superior to the type II fuzzy algorithm. The type II fuzzy control has some problems, such as the slope change on the left wing of MPP point is not obvious, also the optimization range on the right wing of MPP point is narrow. Therefore, the input (slope change rate) of type II fuzzy control is adjusted to duty ratio $D(n-1)$ at $n-1$ moment. At the same time, adding the contraction factor θ to determine the optimal boundary point and PV MPP characteristic curve, makes it more accurate. The method solves the existing problems of tracking speed, stability error and system inertia of type II system.

Table 4 points out that the proposed fuzzy algorithm is superior to type I, II, III and IV fuzzy algorithms in tracking speed, average efficiency, steady-state oscillation rate and steady-state output power, and also proves the feasibility of the proposed algorithm.

Table 4. Comparison of simulation results under 5 fuzzy algorithms

Fuzzy control algorithm	Type I	Type II	Type III	Type IV	Proposed algorithm
Tracking speed(s)	0.083	0.037	0.056	0.070	0.021
Average efficiency (%)	80.43	97.38	96.68	93.78	99.31
Steady state oscillation rate (%)	5.91	2.72	3.43	4.26	0.34
Steady state output/W	740.3	815.8	806.4	780.6	830.8

5. Conclusion

This paper suggests a novel adaptive fuzzy control algorithm that uses the slope of PV P-V characteristic curve and $D(n-1)$ as input, meanwhile introducing contraction factor to adjust $D(n-1)$ in real time. This method makes the optimization range of fuzzy control algorithm wider and maximum power tracking more accurate. Moreover, improving the efficiency of photovoltaic system, stable accuracy and tracking speed are easy to achieve.

The proposed algorithm is compared with type I, II, III and IV fuzzy algorithms. The results show that the proposed algorithm is better than the mentioned fuzzy control algorithms

in optimization range, system inertia and conversion efficiency. In the future, the adaptive variable theory domain fuzzy control algorithm can be adapted to improve the tracking ability and steady oscillation rate of the algorithm.

References

- [1] Khadidja, S., Mountassar, M., & M'hamed, B. (2017, March). Comparative study of incremental conductance and perturb & observe MPPT methods for photovoltaic system. In *2017 International Conference on Green Energy Conversion Systems (GECS)* (pp. 1-6). IEEE.
- [2] Talbi, B., Krim, F., Rekioua, T., Laib, A., & Feroura, H. (2017). Design and hardware validation of modified P&O algorithm by fuzzy logic approach based on model predictive control for MPPT of PV systems. *Journal of Renewable and Sustainable Energy*, 9(4), 043503.
- [3] Harrag, A., & Messalti, S. (2015). Variable step size modified P&O MPPT algorithm using GA-based hybrid offline/online PID controller. *Renewable and Sustainable Energy Reviews*, 49, 1247-1260.
- [4] Abdellatif, W. S., Mohamed, M. S., Barakat, S., & Brisha, A. (2021). A Fuzzy Logic Controller Based MPPT Technique for Photovoltaic Generation System. *International Journal on Electrical Engineering & Informatics*, 13(2).
- [5] Li, X., Wen, H., Hu, Y., & Jiang, L. (2019). A novel beta parameter based fuzzy-logic controller for photovoltaic MPPT application. *Renewable energy*, 130, 416-427.
- [6] Chaouachi, A., Kamel, R. M., & Nagasaka, K. (2010). A novel multi-model neuro-fuzzy-based MPPT for three-phase grid-connected photovoltaic system. *Solar energy*, 84(12), 2219-2229.
- [7] Guenounou, O., Dahhou, B., & Chabour, F. (2014). Adaptive fuzzy controller based MPPT for photovoltaic systems. *Energy Conversion and Management*, 78, 843-850.
- [8] Farajdadian, S., & Hosseini, S. H. (2019). Design of an optimal fuzzy controller to obtain maximum power in solar power generation system. *Solar Energy*, 182, 161-178.
- [9] Ozdemir, S., Altin, N., & Sefa, I. (2017). Fuzzy logic based MPPT controller for high conversion ratio quadratic boost converter. *International Journal of Hydrogen Energy*, 42(28), 17748-17759.
- [10] Ali, M. N., Mahmoud, K., Lehtonen, M., & Darwish, M. M. (2021). Promising MPPT Methods Combining Metaheuristic, Fuzzy-Logic and ANN Techniques for Grid-Connected Photovoltaic. *Sensors*, 21(4), 1244.

- [11] Macaulay, J., & Zhou, Z. (2018). A fuzzy logical-based variable step size P&O MPPT algorithm for photovoltaic system. *Energies*, 11(6), 1340.
- [12] Liu, C. L., Chen, J. H., Liu, Y. H., & Yang, Z. Z. (2014). An asymmetrical fuzzy-logic-control-based MPPT algorithm for photovoltaic systems. *Energies*, 7(4), 2177-2193.
- [13] Loukil, K., Abbas, H., Abid, H., Abid, M., & Toumi, A. (2020). Design and implementation of reconfigurable MPPT fuzzy controller for photovoltaic systems. *Ain Shams Engineering Journal*, 11(2), 319-328.
- [14] Robles Algarín, C., Taborda Giraldo, J., & Rodriguez Alvarez, O. (2017). Fuzzy logic based MPPT controller for a PV system. *Energies*, 10(12), 2036.
- [15] Shiau, J. K., Wei, Y. C., & Chen, B. C. (2015). A study on the fuzzy-logic-based solar power MPPT algorithms using different fuzzy input variables. *Algorithms*, 8(2), 100-127.
- [16] Priyadarshi, N., Azam, F., Bhoi, A. K., & Alam, S. (2019). An artificial fuzzy logic intelligent controller based MPPT for PV grid utility. In *Proceedings of 2nd International Conference on Communication, Computing and Networking* (pp. 901-909). Springer, Singapore.
- [17] Ganthia, B. P., Pradhan, R., Das, S., & Ganthia, S. (2017, August). Analytical study of MPPT based PV system using fuzzy logic controller. In *2017 International Conference on Energy, Communication, Data Analytics and Soft Computing (ICECDS)* (pp. 3266-3269). IEEE.
- [18] Talbi, B., Krim, F., Rekioua, T., Laib, A., & Feroura, H. (2017). Design and hardware validation of modified P&O algorithm by fuzzy logic approach based on model predictive control for MPPT of PV systems. *Journal of Renewable and Sustainable Energy*, 9(4), 043503.
- [19] Kumar, N. K., & Gandhi, V. I. (2019). Implementation of fuzzy logic controller in power system applications. *Journal of Intelligent & Fuzzy Systems*, 36(5), 4115-4126.
- [20] Chandramouli, A., & Sivachidambaranathan, V. (2019). Extract maximum power from PV system employing MPPT with FLC controller. *power*, 1(4).